Energy-driven subunit rotation at the interface between subunit a and the c oligomer in the F_O sector of *Escherichia coli* ATP synthase

Marcus L. Hutcheon, Thomas M. Duncan, Helen Ngai, and Richard L. Cross*

Department of Biochemistry and Molecular Biology, State University of New York Upstate Medical University, Syracuse, NY 13210

Communicated by Paul D. Boyer, University of California, Los Angeles, CA, May 14, 2001 (received for review April 4, 2001)

Subunit rotation within the F_1 catalytic sector of the ATP synthase has been well documented, identifying the synthase as the smallest known rotary motor. In the membrane-embedded F_O sector, it is thought that proton transport occurs at a rotor/stator interface between the oligomeric ring of c subunits (rotor) and the single-copy a subunit (stator). Here we report evidence for an energy-dependent rotation at this interface. F_OF_1 was expressed with a pair of substituted cysteines positioned to allow an intersubunit disulfide crosslink between subunit a and a c subunit [aN214C/cM65C; Jiang, W. & Fillingame, R. H. (1998) *Proc. Natl. Acad. Sci. USA* 95, 6607–6612]. Membranes were treated with *N,N′*-dicyclohexyl-[^{14}C]carbodiimide to radiolabel the D61 residue on less than 20% of the c subunits. After oxidation to form an a–c crosslink, the c subunit properly aligned to crosslink to subunit a was found to contain very little ^{14}C label relative to other members of the c ring. However, exposure to MgATP before oxidation significantly increased the radiolabel in the a–c crosslink, indicating that a different c subunit was now aligned with subunit a. This increase was not induced by exposure to MgADP/P_i. Furthermore, preincubation with MgADP and azide to inhibit F_1 or with high concentrations of *N,N′*-dicyclohexylcarbodiimide to label most c subunits prevented the ATP effect. These results provide evidence for an energy-dependent rotation of the c ring relative to subunit a.

H^+-transporting, F_OF_1-ATP synthases (reviewed in refs. 1–5) are found in the membranes of eubacteria, mitochondria, and chloroplasts, where they catalyze the synthesis of ATP from ADP and P_i during oxidative- or photo-phosphorylation. The F_1 sector, which contains the catalytic nucleotide binding sites for ATP synthesis, can be removed from the membrane as a water-soluble complex that functions as an ATPase. The F_O sector remains embedded within the membrane and, in the absence of F_1, conducts passive H^+ transport across the bilayer. The minimal subunit composition of F_OF_1 is represented by the *Escherichia coli* synthase, in which F_1 has five subunits with the stoichiometry $\alpha_3\beta_3\gamma\delta\varepsilon$, and F_O has three subunits with the stoichiometry ab_2c_{9-12} (6).

Data from many experimental approaches support the general structural model for F_OF_1 shown in Fig. 1. For the F_1 sector, high-resolution structures are available (7–9). The arrangement of subunits in F_O is supported by studies with electron microscopy (10) and atomic force microscopy (11, 12). A recent low-resolution x-ray structure for an F_1c_{10} subcomplex from yeast mitochondrial synthase (13) supports the oligomeric packing of c subunits in a ring, as well as the interactions of γ and ε with the polar surface of the ring, as indicated by earlier genetic and subunit crosslinking studies (14–17).

ATP synthase uses the transport of H^+ (or in some cases Na^+, see ref. 18) down a transmembrane, electrochemical gradient to drive net ATP synthesis. Under certain conditions, this coupling process can run in reverse as an ATPase-driven proton (or sodium) pump. The mechanism by which the ATP synthase catalyzes efficient, reversible energy coupling between vectorial ion transport and the chemical reactions of ATP synthesis/hydrolysis has been a major focus of research in bioenergetics. The binding change mechanism provides a model that best accommodates a broad range of experimental results (19, 20). It states that energy from proton transport through F_O indirectly drives net ATP synthesis by inducing cyclical conformational changes between tight substrate binding and product release at three alternating, cooperative catalytic sites on F_1 (21, 22). It further proposes that these binding changes are driven by the rotation of an asymmetric core (γ in Fig. 1) relative to the three surrounding catalytic subunits (β) (23).

The structure of F_1 at atomic resolution showed that γ determines the conformational states of the three catalytic subunits (7), consistent with a rotary mechanism. Subsequent studies with isolated F_1-ATPase (24–26) documented catalysis-dependent rotation of γ relative to the catalytic β subunits. A disulfide-crosslinking approach indicated that rotation of γ also occurs in membrane-bound F_OF_1 during ATP hydrolysis (27) and synthesis (28). Finally, it was shown that, during ATP hydrolysis, ε also moves with γ as part of the central rotor in F_1 (29) as well as in membrane-bound F_OF_1 (30).

In coupling proton transport to ATP synthesis, most recent models predict that subunit rotation also occurs within F_O (see refs. 1 and 31–33). The two motors, F_1 and F_O, are thought to share a common rotor ($\gamma\varepsilon c_{9-12}$) and a peripheral stator ($b_2\delta$) so that proton-driven rotation in F_O forces γ to rotate within F_1, thereby driving the binding changes required for ATP synthesis (Fig. 1). Recent experiments indicate that the c ring moves with $\gamma\varepsilon$ as part of the rotor in F_OF_1. Coupled functions of *E. coli* F_OF_1 were not blocked by an ε-c disulfide linkage (34) nor by the combined γ-ε-c disulfide linkages (35). With detergent-extracted *E. coli* F_OF_1, anchored to a solid surface by affinity tags on the α subunits, an actin filament attached to the c ring was observed to rotate by fluorescence microscopy (36). However, the functional significance of this observation is controversial (37), because rotation was insensitive to specific inhibitors of F_O function. Furthermore, the results suggest a rotation of the c ring relative to the immobilized $\alpha_3\beta_3$ complex, but do not provide information regarding possible rotation relative to other F_O subunits. The first direct indication of relative subunit rotation within F_O has come from a recent crosslinking study. Exchange of c subunits at the interface of the c ring with b_2 indicates rotation of the c ring vs. b_2, but again it was not possible to demonstrate energy-dependent rotation (38).

Extensive genetic studies (ref. 39 and reviewed in refs. 32 and 40) have long suggested that subunits a and c function together to transport protons. Rotation of the c ring relative to subunit a could explain how a single copy of a can coordinate this function with multiple copies of c. Detailed models for such a rotary transport mechanism have been presented (5, 24, 31, 41–45) but,

Abbreviations: DCCD, *N,N′*-dicyclohexylcarbodiimide; NEM, *N*-ethylmaleimide.

*To whom reprint requests should be addressed. E-mail: crossr@mail.upstate.edu.

The publication costs of this article were defrayed in part by page charge payment. This article must therefore be hereby marked "*advertisement*" in accordance with 18 U.S.C. §1734 solely to indicate this fact.

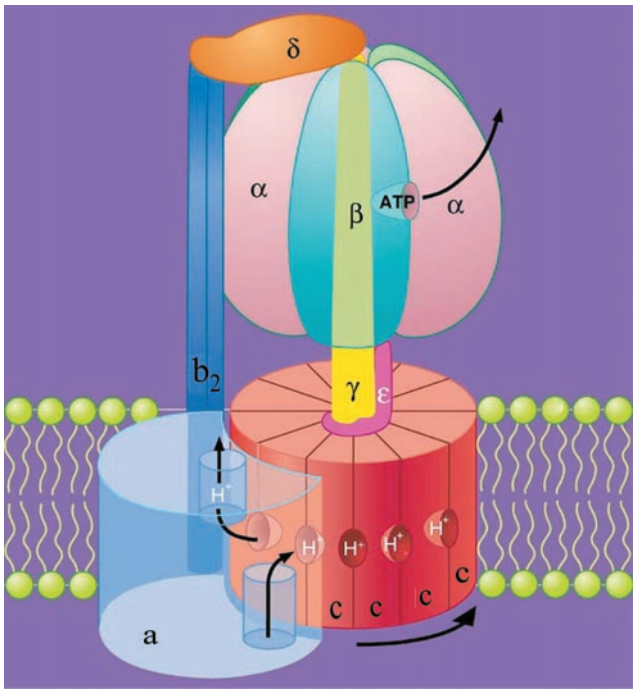

Fig. 1. Model for the structure and mechanism of *E. coli* F_OF_1. Adapted from Duncan *et al.* (24). The membrane-embedded F_O sector catalyzes proton transport and consists of one copy of subunit a, a dimer of b subunits, and an oligomeric ring of c subunits. The hydrophilic F_1 sector extends ≈120 Å from the cytoplasmic face of the membrane and contains five subunits with the stoichiometry $\alpha_3\beta_3\gamma_1\delta_1\varepsilon_1$. The α and β subunits alternate in a hexamer that surrounds a central asymmetric core consisting of the γ subunit. Three catalytic nucleotide-binding sites (one visible) are located at alternate α/β subunit interfaces, primarily on the β subunits. F_1 binds to F_O through two distinct linkages: (*i*) a central stalk (or rotor) comprised of $\gamma\varepsilon$ and anchored to the c ring, and (*ii*) a peripheral stalk (or stator), comprised of $b_2\delta$, that anchors $\alpha_3\beta_3$ to the a subunit. Two partial channels for proton transport, each accessible to a different side of the membrane, are thought to be located between the a and c subunits. During ATP synthesis, each proton would enter through the periplasmic channel and bind to a deprotonated c subunit. The c ring then would rotate one step to the right relative to subunit a, and net transport would occur as a previously protonated c subunit moves into alignment with the cytoplasmic channel and loses its proton. Because the c ring is anchored to $\gamma\varepsilon$ and subunit a is tethered to $\alpha_3\beta_3$ by $b_2\delta$, rotation of the c ring relative to subunit a forces γ to rotate relative to the catalytic subunits, thus driving the binding changes required to achieve net synthesis of ATP.

as yet, there is no direct evidence that the c ring rotates relative to subunit a.

Here we focus on the interface between subunit a and the c ring, with the goal of testing whether energy-dependent subunit rotation may occur. Our strategy required the ability to form an a–c disulfide crosslink as a means of identifying the particular c subunit that is adjacent to subunit a, combined with an ability to asymmetrically tag the c subunits. An energy-dependent change in the amount of label associated with the c subunit that can be trapped in the a–c crosslinked product then would indicate a rotation of the c ring relative to subunit a. A recent exhaustive topological study involving intersubunit disulfide crosslinking of pairs of substituted cysteine identified points of contact between subunit a and an adjacent subunit c (43). One such contact point involved the aN214C/cM65C cysteine pair, which we chose for our study because of its high crosslinking yield (43). As a means of tagging the c subunits, we chose minimal labeling by *N*,*N*′-dicyclohexyl-[^{14}C]-carbodiimide ([^{14}C]DCCD). Subsequent formation of the a–c crosslink in membrane-bound F_OF_1 showed that the c subunit in the a–c crosslinked product was largely protected from reaction with [^{14}C]DCCD relative to other c subunits. However, exposure to conditions for ATP-driven catalytic turnover before crosslinking resulted in a significant increase in ^{14}C in the a–c band. These results provide evidence for an energy-dependent rotation of the c ring relative to subunit a.

Experimental Procedures

Materials. *N*-ethylmaleimide (NEM), *p*-trifluoro-methoxyphenylhydrazone (FCCP), ATP, ADP, asolectin, taurodeoxycholic acid, and sodium azide were from Sigma. *p*-Aminobenzamidine dihydrochloride was from Aldrich. Phenylmethylsulfonyl fluoride was from American Bioanalytical. [^{14}C]DCCD (≈54 mCi/mmol) and ^{125}I-labeled IgG (goat) against rabbit Ig were obtained from Amersham Pharmacia. SYPRO orange dye was from Molecular Probes. Poly(vinylidene difluoride) blotting membranes were from Invitrogen. Polyacrylamide gels for SDS/PAGE (Tris-HCl Ready gels, 4–15% acrylamide) were from BioRad. Pyruvate kinase (rabbit) and lactate dehydrogenase (pig) (each 10 mg/ml in 50% glycerol) were from Roche Diagnostics. Polyclonal rabbit antibodies against subunits a (46) and c (47) were provided by R. H. Fillingame, University of Wisconsin, Madison. Other reagents and chemicals were of the highest grade available.

Plasmids and *E. coli* Strains. Dr. Fillingame's laboratory kindly supplied plasmids pYZ201, pYZ217 (pYZ201 containing cQ42C; ref. 15), and pDF163 constructs containing the combined mutations aN214C/cM65C (43) or aN214C/cQ42C/cM65C (constructed by Weiping Jiang, University of Wisconsin, Madison). To allow optimal overexpression of F_OF_1 containing these mutations, the mutant *uncBE* genes (for subunits a and c, respectively) were transferred from the above constructs into the high copy number construct pJW1, which encodes the genes for all eight subunits of F_OF_1 (48). Each pDF163 construct was first converted to a pYZ201 construct by inserting the 6.95-kb *Sph*I fragment from wild-type pYZ201 into pDF163's unique *Sph*I site, in the desired orientation (*uncBEFHAGDC*). The 4.4-kb *Hin*dIII fragment (*uncBEFHAG′*) of each mutant pYZ201 was then used to replace the same wild-type fragment in pJW1. All cloning procedures followed standard protocols. The final clones, pJW1-cQ42C, pJW1-aN214C/cM65C, and pJW1-aN214C/cQ42C/cM65C, were transformed into the expression strain AN887, in which the chromosomal *unc* operon is inactivated (49). Cells were grown in volumes up to 12 liters in defined medium with appropriate supplements (50), including 0.05–0.1 mg ampicillin/ml, 40% Luria broth, 60 mM glucose, and 1% (vol/vol) glycerol.

Preparation of Membranes. All steps were done at 4°C, and the pH of each buffer was adjusted at 4°C unless otherwise noted. Membranes were prepared as described (48), stopping after the final wash with buffer containing *p*-aminobenzamidine. Using purified F_OF_1 as a standard on SDS/PAGE, stained α and β subunits and immunodetection of subunit a all indicated that F_OF_1 accounted for ≈50% of total membrane protein. F_1-depleted membranes were prepared by exposure to 2 mM Tris·HCl, 1 mM EDTA, pH 8.0, with subsequent collection of the membranes by ultracentrifugation. These steps were repeated once, with final resuspension of membranes in MTGMg8 buffer [50 mM Mops-Tris/10% glycerol (vol/vol)/2 mM $MgCl_2$, pH 8.0, room temperature]. This procedure removed >97% of the ATPase activity of the membranes.

Reaction of Membranes with [^{14}C]DCCD and Induction of an Intersubunit, a–c Disulfide Crosslink. Aliquots of [^{14}C]DCCD in toluene (53.9 μCi/ml) were dried by using a Savant Speedvac, dissolved at ≈1 mM in dry DMSO, and stored at −20°C. Membranes (1 mg protein/ml) were treated with [^{14}C]DCCD (10–100 μM, as

noted) in MTGMg8 buffer for up to 2 h at room temperature. Aliquots were removed for immediate coupled-enzyme assays of ATPase. An aliquot also was taken to determine total covalent ^{14}C labeling of proteins as described below. Immediately after reaction with [^{14}C]DCCD, aliquots were diluted to 0.5 mg/ml with MTGMg8 buffer containing additional $MgCl_2$ (5 mM final) and 2 μM *p*-trifluoro-methoxyphenylhydrazone (FCCP) (except as noted). For most samples, an equal volume of buffer containing either ADP/P_i or ATP was added with vortexing (4 mM final ADP/P_i or ATP). An additional variation was the addition of ADP/azide (1 mM each, final) during the second hour of DCCD treatment, followed by dilution with buffer containing ATP as above. For ATP synthesis conditions, 5 mM or 12 mM $MgCl_2$ was used, FCCP was omitted, and samples were preincubated with succinate (2.5 mM) for 4 min to establish a transmembrane proton motive force. ADP and P_i (4 mM/20 mM final) were then added and the sample was incubated for 2–3 min at room temperature. Finally, I_2 was added (50 μM final), and samples were incubated for 10 min to induce a–c crosslinking. To maintain consistency in the oxidation potential, I_2 was diluted to 1 mM with MTGMg8 from a 0.2 M stock in dry ethanol just before addition to each sample. Each reaction was quenched by mixing a 7:3 volume ratio of sample with 4× gel sample buffer (51) containing 5 mM NEM to block cysteines.

SDS/PAGE, SYPRO Orange Staining, and Detection of Relative ^{14}C Incorporation. Samples (typically 8 μg protein/lane) were electrophoresed (51) on a 4–15% polyacrylamide gradient gel. The gel was soaked in water for 10 min, then stained with 50 ml of SYPRO orange [1:5,000 dilution in 7.5% glacial acetic acid (vol/vol)] for 45 min. The gel was destained with 7.5% (vol/vol) acetic acid for 25 min, and then placed in water for 30 min. Protein bands with bound SYPRO orange were imaged by scanning the gel with a STORM 860 (Molecular Dynamics) in blue fluorescent mode. The gel was then vacuum-dried on filter paper and exposed to a low-energy storage phosphor screen (Molecular Dynamics) for 40–120 h to detect ^{14}C-containing bands. The exposed screen was then scanned on the STORM 860 in the phosphorimage mode at 650 nm. IMAGEQUANT 5.1 software (Molecular Dynamics) was used for data analysis. For analysis of ^{14}C label in components of the a–c band, a gel slice containing the band was macerated and incubated for 2 h at 30°C with a minimal volume of 1× gel sample buffer containing β-mercaptoethanol and 50 mM DTT. The sample was then centrifuged and the supernatant was loaded on a 4–15% Ready gel for separation of proteins. The gel was stained with SYPRO orange to reveal residual, unreduced a–c product as well as a- and c-subunit bands. The gel was then dried and exposed to a low-energy storage phosphor screen for ≈210 h to quantitate ^{14}C.

Detection of Subunits a and c by Immunoblotting. Electrophoresis was performed as above, with 4 μg of membrane protein loaded per lane. Protein bands were transferred to a poly(vinylidene difluoride) membrane as described (27), with 0.25 A of constant current for 75 min. Immunoblotting followed a previous protocol (30). Incubation with anti-a or anti-c rabbit antibody (1:5,000) was for 2 h. Incubation with ^{125}I-labeled anti-rabbit-Ig antibody was for 1.5 h. After the final rinse, the blot was dried and exposed to a standard phosphor screen (Molecular Dynamics) for 20–24 h. The exposed screen was scanned and analyzed as noted above.

Other Assays. To determine total covalent incorporation of ^{14}C into proteins after treatment of membranes with [^{14}C]DCCD, protein was precipitated with deoxycholate and trichloroacetic acid (52), the pellet was washed with 0.5 ml of cold trichloroacetic acid (10%, wt/vol) and resuspended in gel sample buffer lacking reductant. Aliquots were then taken for scintillation counting and protein determination. Control experiments with F_OF_1 liposomes (not shown) confirmed that all F_OF_1 subunits were precipitated and recovered equally by this procedure. For liquid scintillation counting of ^{14}C, each sample was added to a vial containing 4 ml of Biosafe-II scintillant and 0.5 ml of water, then counted in a Beckman LS-6500. Protein was determined by a modified Lowry assay (52). ATPase activity was measured at 30°C, pH 8, with a spectrophotometric, coupled-enzyme assay as described (30). Assay conditions included 6 mM $MgCl_2$, 5 mM ATP, 10 μM *p*-trifluoro-methoxyphenylhydrazone (FCCP), and 5 mM KCN. In some experiments, 0.5% lauryl dimethylamine oxide was added to assays to uncouple F_1 from F_O (53) and thus determine whether any inhibition of ATPase was caused by direct modification of F_1 subunits by [^{14}C]DCCD. The uncoupled F_1-ATPase activity was essentially unaffected by treatment of membranes with 10 μM [^{14}C]DCCD for 2 h, but was inhibited ≈5% by treatment with 100 μM [^{14}C]DCCD for 0.5 h.

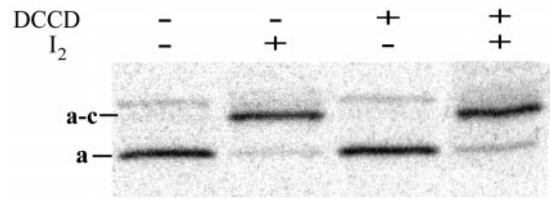

Fig. 2. Anti-a immunoblotting analysis of aN214C/cM65C-membranes. As indicated above the lanes, aliquots of aN214C/cM65C-membranes were incubated with or without 10 μM DCCD for 2 h, then with or without 50 μM I_2 for 10 min. Samples were subjected to nonreducing SDS/PAGE and transferred to a poly(vinylidene difluoride) membrane. Immunodetection of bands containing subunit a was performed as described in *Experimental Procedures*. Nonoxidized samples show a minor immunoreactive band just above the position of migration of the a–c band that becomes smeared upon oxidation. This band is not observed on immunoblots of isolated F_OF_1 in liposomes (not shown). See Table 1 for quantitation of crosslinking.

Results

Iodine was used to induce crosslinking of aN214C to cM65C in *E. coli* membranes. The identity of the a–c crosslink band on SDS/PAGE was confirmed by immunoblotting using the same antibodies against a (Fig. 2) and c (data not shown) as used by Jiang and Fillingame (43). Incubation with 50 μM I_2 for 10 min (>97% crosslinking; Fig. 2, lane 2 and Table 1) was much more effective than incubation for 1 h with copper phenanthroline (<40% crosslinking; ref. 43).

With the ability to crosslink subunit a to a properly aligned c subunit, our next goal was to obtain differential labeling of the c subunits so that the proximal c subunit could be distinguished from others in the c ring. It had been previously reported that the cQ42C substitution in the subunit's polar loop allowed rapid

Table 1. Yields of a–c crosslinking in aN214C/cM65C-membranes and the effects of DCCD treatment

DCCD treatment*	Efficiency of a–c crosslinking†
None	>97%
10 μM, 2 h‡	96.5% (±0.4%)
100 μM, 0.5 h	81.4% (±0.7%)

*Similar experiments with [^{14}C]DCCD showed labeling of 1.8 c/F_OF_1 for 10 μM [^{14}C]DCCD and 9 c/F_OF_1 for 100 μM [^{14}C]DCCD (Table 2).

†Crosslinking efficiency (±SD) was estimated from immunoblot detection of subunit a (see Fig. 2). Controls using varied amounts of nonoxidized sample established that the assay provided a linear response to subunit a for the amounts remaining in oxidized samples.

‡Exposure to MgATP before crosslinking had no significant effect on the yield of a–c product.

Table 2. [^{14}C]DCCD inhibition and labeling of aN214C/cM65C-F_OF_1 in membranes

Treatment	Inhibition of ATPase (%)*	^{14}C-labeled c subunits [mol/mol F_OF_1]†
10 μM [^{14}C]DCCD, 2 h	74% (±5)	1.8 (±0.2)
100 μM [^{14}C]DCCD, 0.5 h	92% (±1)	9.1 (±0.3)

*Inhibition was measured relative to a sample incubated in parallel without [^{14}C]DCCD. Values for inhibition (±SD) are from six (10 μM) or three (100 μM) experiments. Note that treatment with 100 μM [^{14}C]DCCD caused ~5% direct inhibition of F_1 activity, as measured in the presence of 0.5% lauryl dimethylamine oxide.

†Distribution of ^{14}C in SDS/PAGE samples was determined by PhosphorImager scanning (see Fig. 3). A low-level baseline was subtracted for the entire lane. Excluding the ''free'' [^{14}C]DCCD peak, the sum of all significant peak areas is assumed to correspond to the total incorporated ^{14}C determined by scintillation counting. For nonoxidized samples, the c peak accounted for 93% or 81% of total ^{14}C incorporated after reaction with 10 or 100 μM [^{14}C]DCCD, respectively. The standard deviations shown only reflect experimental reproducibility. Actual stoichiometries may have greater uncertainty due to errors in the measured F_OF_1 content of membranes, in the specific activity of the [^{14}C]DCCD, in the assumed molecular weight of F_OF_1 (based on 10 c/mol), and in the method of background subtraction.

[^{14}C]NEM labeling of about 60% of c subunits in F_OF_1, whereas the other 40% was labeled at a much slower rate (54). Based on the possibility that subunit a might in part determine this biphasic labeling, we treated F_OF_1 liposomes containing the aN214C/cM65C/cQ42C mutations with [^{14}C]NEM. As expected (55), controls with aN214C/cM65C-F_OF_1 liposomes showed that the membrane-embedded Cys residues were much less reactive toward [^{14}C]NEM than was cQ42C. Consequently, the yields of a–c crosslinking with aN214C/cM65C/cQ42C-F_OF_1 liposomes were not significantly decreased by labeling a fraction of c subunits at cQ42C. However, even under mild conditions that labeled only one cQ42C/F_OF_1, there was no evidence of asymmetry in the ^{14}C content of c subunits relative to the specific c subunit that could form the a–c crosslink upon oxidation.

As an alternative approach, we reasoned that c-subunit residues at the a/c interface might be less accessible to modification by hydrophobic reagents than those exposed to lipids (see Fig. 1). To test this possibility, we treated the enzyme with [^{14}C]DCCD to label c subunits at cD61. This residue appears to reside near the center of the bilayer (2, 56), one α-helical turn from the cM65C residue used to form the a–c crosslink. Incubation of membranes containing the aN214C/cM65C mutant pair with 10 μM [^{14}C]DCCD for 2 h resulted in the labeling of 1.8 c subunits per F_OF_1 (Table 2). The distribution of ^{14}C label among protein bands on SDS/PAGE is shown in Fig. 3*A*. High specificity for labeling c subunits is evident, as the c band accounted for >90% of all ^{14}C incorporated. A small amount of ^{14}C was present at the position of a–c even in nonoxidized samples (Fig. 3*A*, black trace), but immunoblotting indicated that <5% of subunit a was present at that position before oxidation (Fig. 2). If the labeling of c subunits with [^{14}C]DCCD was random, then after oxidation, the single c subunit in the a–c band should contain ≈10% of the total ^{14}C incorporated, assuming 10 copies of c per F_O (13, 57). However, only a small increase in ^{14}C was detected in the a–c band of oxidized samples (green trace). After subtracting the background radioactivity at the a–c position for a nonoxidized control, the a–c crosslinked product contained only 1.2% (±0.3) of the total ^{14}C bound to c subunits. This value is 8-fold less than expected from random labeling of subunits within the c ring.

One trivial explanation for the low level of labeling of the a–c crosslinked product that would still be consistent with random labeling of c subunits would be that DCCD modification of cD61 prevents cM65C from crosslinking to aN214C. If this was the case, then the labeling of about 20% of the c subunits would result in a 20% decrease in the yield of the a–c crosslinked product. However, quantitation of subunit a in the a and a–c bands of immunoblots does not support this possibility. The crosslinking yield was decreased by less than 4% by labeling with 10 μM DCCD (Table 1). Furthermore, after treating membranes with 100 μM DCCD to label most of the c subunits (Table 2), the a–c crosslinking yield decreased by less than 20% (Table 1), whereas the ^{14}C in the a–c band was ≈10-fold less than expected

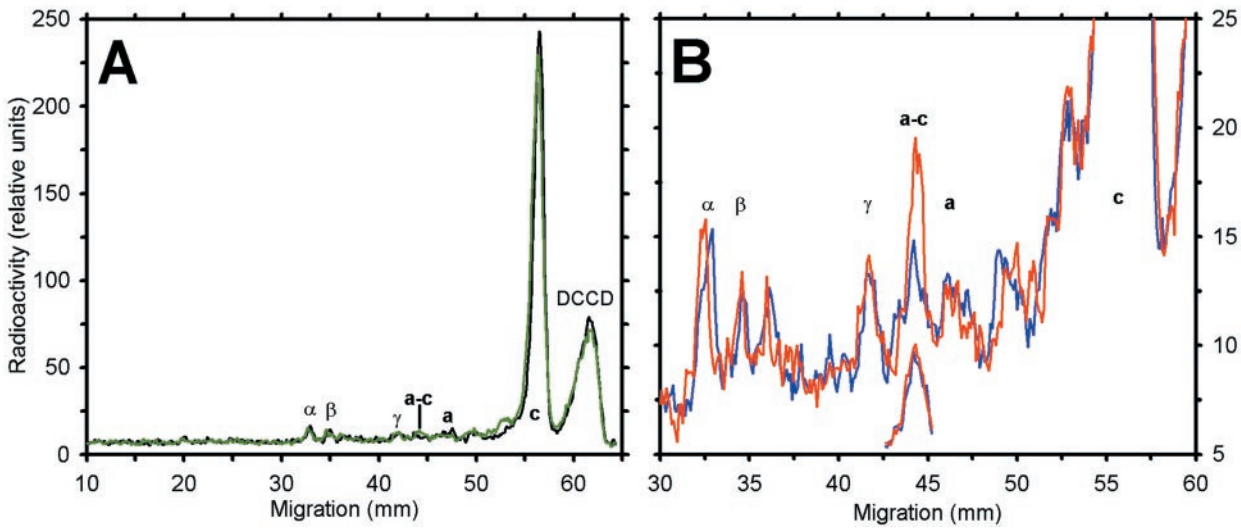

Fig. 3. Distribution of incorporated ^{14}C from SDS/PAGE analysis of [^{14}C]DCCD-treated aN214C/cM65C-membranes. A membrane sample (1 mg protein/ml) was incubated for 2 h with 10 μM [^{14}C]DCCD, resulting in 72% inhibition of ATPase activity. Aliquots were diluted and exposed to different conditions for 3 min, then incubated alone or with 50 μM I_2 for 10 min. Each aliquot then was denatured in the presence of 5 mM NEM and analyzed by nonreducing SDS/PAGE. The dried gel was exposed to a storage phosphor screen for ≈6 days. Shown are the profiles of radioactivity in sample lanes after scanning the phosphor screen. Locations of F_OF_1 subunits are noted. (*A*) Nonoxidized (black) and oxidized (green) controls. The peak at the migration front (labeled DCCD), represents [^{14}C]DCCD that hydrolyzed or reacted with a buffer component. (*B*) Comparison of aliquots exposed to 4 mM ADP/P_i (blue) or 4 mM ATP (red) before oxidation. The offset, partial traces show the radiolabel in the a–c band for a sample treated with 100 μM [^{14}C]DCCD for 0.5 h before the nucleotide incubation and oxidation steps noted above. The scale for the offset traces is about 3-fold greater than that shown on the *y* axis.

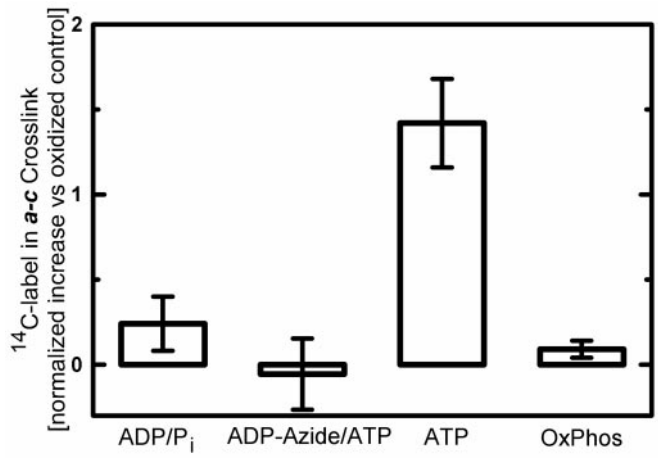

Fig. 4. Effects of nucleotides and energization on the amount of [^{14}C]DCCD-labeled c subunit in the a–c crosslink with aN214C/cM65C-membranes. Membranes were treated with 10 μM [^{14}C]DCCD to covalently label ≈2 c subunits/F_OF_1. Aliquots were then exposed to the conditions indicated before oxidation by I_2 to induce a–c crosslinking. Samples were subjected to nonreducing SDS/PAGE, and the relative amounts of ^{14}C in the c and a–c bands were determined. Anti-a immunoblots showed that the efficiency of a–c crosslinking was consistent from sample to sample. The ^{14}C content of the a–c band from an oxidized control lacking exposure to nucleotides was subtracted from the a–c value for each experiment. To average the results of independent experiments, data were normalized to the total counts in the c band of the nonoxidized controls. Thus, results for a–c bands are presented as a percentage of the total ^{14}C in the c subunits. The oxidized controls subtracted averaged 2.1% (±0.2) for the a–c band. Values shown (±SE bars) are the means from six replicates (ADP/Pi, ATP, and OxPhos) or three replicates (ADP-Azide/ATP). Unpaired t tests indicate clear statistical differences for exposure to ADP/P_i or ADP-Azide/ATP vs. ATP ($P < 0.01$ each) and for ATP vs. conditions for oxidative phosphorylation (OxPhos, $P < 0.001$).

for random labeling of c subunits (data not shown). These results clearly indicate that the c subunit capable of forming the a–c crosslink is much less reactive toward DCCD than other c subunits in the c ring.

The asymmetric labeling of c subunits with [^{14}C]DCCD thus allows the c subunit that can crosslink to subunit a to be distinguished from others in the c ring. Although DCCD modification of one or more c subunits inhibits rapid catalysis detectable by normal assays (Table 2 and ref. 58), it seemed plausible that conditions for ATP hydrolysis might drive a limited rotation of the c ring relative to subunit a and so bring a labeled c subunit into alignment with subunit a. Hence, membranes expressing aN214C/cM65C were treated with 10 μM [^{14}C]DCCD to label about 2 c/F_OF_1 and then exposed to different conditions before oxidation to form the a–c crosslink. Fig. 3*B* compares the distribution of ^{14}C on an SDS/PAGE gel for a labeled membrane sample that was divided and treated for 2 min with either MgADP/P_i (blue trace) or MgATP (red trace) before oxidation to form the a–c crosslink. Treatment with MgATP caused a significant increase in the amount of ^{14}C present in the a–c band. To be certain that the increase was caused by an increase in ^{14}C associated with the c subunit, a–c bands were extracted, reduced, and reanalyzed by SDS/PAGE. In the absence of ATP before oxidation, the a and c bands released from the a–c crosslink showed similar low levels of ^{14}C. For the sample exposed to MgATP just before oxidation, the level of ^{14}C in the a band was unchanged, but the c band showed a 2-fold increase (data not shown). Similar results were obtained by using F_OF_1 liposomes. Thus, the ATP-induced increase observed (Figs. 3*B* and 4) was caused by an increase in ^{14}C-labeled c subunit in the a–c crosslinked product, indicating that a different c subunit had moved into alignment with subunit a.

The MgATP-dependent increase observed was less than one-fourth of that expected if catalysis-dependent rotation of the c ring had completely randomized the position of ^{14}C-labeled c subunits relative to subunit a. Several factors may contribute to this less-than-maximal response. First, steric hindrance by the incorporated probe may kinetically limit the entry of labeled c subunits into the a/c interface. Second, a fraction of the F_OF_1 may be inhibited by MgADP and thus incapable of ATP-driven subunit rotation. Finally, only c rings with a single modified c subunit may have sufficient rotational mobility to move the labeled c into alignment with subunit a. The latter explanation is consistent with the fact that preincubation with 100 μM [^{14}C]DCCD to modify most c subunits completely prevented the ATP effect (Fig. 3*B*, offset traces for the a–c peak).

Fig. 4 summarizes results from several experiments in which membranes were labeled by 10 μM [^{14}C]DCCD. Consistently, the ^{14}C present in the a–c crosslinked product was greater after exposure to MgATP. No such increase was seen after exposure to ADP/P_i or when samples were preincubated with inhibitory MgADP/azide before addition of MgATP. Hence, the movement of DCCD-labeled c subunits into the a/c interface requires conditions for ATP hydrolysis by F_OF_1.

Conditions for oxidative phosphorylation before crosslinking also were tested. However, in this case, no change in the ^{14}C present in the a–c band was observed compared with the control (Fig. 4). H^+-pumping assays done with aN214C/cM65C-membranes confirmed that succinate was an effective substrate for generating a transmembrane pH gradient, and vigorous aeration before crosslinking confirmed that oxygen was not limiting under conditions for oxidative phosphorylation (data not shown).

Discussion

The experiments presented here provide direct evidence that c subunits rotate relative to subunit a in membrane-bound F_OF_1. Although the approach used cannot show a complete or unidirectional cycle of rotation, the results are strongly supportive of energy coupling models that postulate direct rotary coupling between F_O and F_1, in which the rotor consists of the c ring plus $\gamma\varepsilon$ and the stator of $ab_2\delta$ plus $\alpha_3\beta_3$ (Fig. 1). Furthermore, we show that subunit rotation at the a/c interface is energy-driven.

DCCD is a well-known inhibitor of the ATP synthase. Extensive modification of c subunits with 50 or 100 μM DCCD inhibits rotation of the c ring relative to subunit b (38), rotation of γ relative to $\alpha_3\beta_3$ (28), and rotation of the c ring relative to subunit a (Fig. 3*B*, offset traces). Hence, at high labeling stoichiometries, DCCD appears to cause total seizure in the F_O motor. Even at low labeling stoichiometries, DCCD inhibits catalytic activity measured by standard assays that have detection limits in the hundreds of ATP hydrolyzed per min per F_OF_1 (58). However, to detect subunit rotation by the approach used here, only one or two turnovers are required per F_OF_1 during the 2-min incubation with MgATP. Figs. 3 and 4 demonstrate that such limited subunit rotation can be driven by ATP hydrolysis when less than 20% of the c subunits are modified.

We were unable to demonstrate proton-driven subunit rotation under conditions for ATP synthesis. One possible explanation relates to the fact that ATP synthesis rates are typically much lower than ATPase rates for *E. coli* membranes (28, 59). Hence the lack of a detectable response may be due to the presence of a smaller fraction of active F_OF_1 complexes under ATP synthesis conditions. A second possibility relates to the fact that the c ring would be expected to rotate in the opposite direction from that obtained under ATP hydrolysis conditions. Hence a DCCD-

modified c subunit may run into a greater physical barrier than that encountered when it enters the a/c interface from the other direction.

The asymmetric labeling of the c ring merits further comment. The c subunit capable of forming the aN214C-cM65C crosslink is strongly resistant to reaction with DCCD relative to other subunits in the c ring (Table 1, Fig. 3*A*). This may be the result of reduced access of DCCD to the a/c interface due to polarity and/or steric effects. Alternatively, because DCCD reacts with protonated carboxyls (60), the c subunit aligned to crosslink to subunit a may be in the deprotonated state. This would be consistent with a docking model for the a/c ring (45), in which aN214 is proximal to cM65 of the deprotonated c subunit.

We thank Dr. Robert Fillingame and his associates of the University of Wisconsin for both supplying antibodies and plasmids and for helpful discussions. We also thank Dr. Ron Kaback of the University of California, Los Angeles for suggesting I_2 as an effective oxidant for membrane-embedded Cys and Drs. Yakov Milgrom and Vladimir Bulygin for helpful discussions. Ms. Pei Lin assisted in a number of preliminary experiments. This work was supported by Grant GM23152 from the National Institutes of Health, U.S. Public Health Service.

1. Junge, W. (1999) *Proc. Natl. Acad. Sci. USA* **96,** 4735–4737.
2. Fillingame, R. H., Jiang, W., Dmitriev, O. Y. & Jones, P. C. (2000) *Biochim. Biophys. Acta* **1458,** 387–403.
3. Kinosita, K., Jr., Yasuda, R., Noji, H. & Adachi, K. (2000) *Philos. Trans. R. Soc. London B* **355,** 473–489.
4. Leslie, A. G. & Walker, J. E. (2000) *Philos. Trans. R. Soc. London* **355,** 465–471.
5. Oster, G. & Wang, H. (2000) *Biochim. Biophys. Acta* **1458,** 482–510.
6. Foster, D. L. & Fillingame, R. H. (1982) *J. Biol. Chem.* **257,** 2009–2015.
7. Abrahams, J. P., Leslie, A. G., Lutter, R. & Walker, J. E. (1994) *Nature (London)* **370,** 621–628.
8. Bianchet, M. A., Hullihen, J., Pedersen, P. L. & Amzel, L. M. (1998) *Proc. Natl. Acad. Sci. USA* **95,** 11065–11070.
9. Gibbons, C., Montgomery, M. G., Leslie, A. G. & Walker, J. E. (2000) *Nat. Struct. Biol.* **7,** 1055–1061.
10. Birkenhager, R., Hoppert, M., Deckers-Hebestreit, G., Mayer, F. & Altendorf, K. (1995) *Eur. J. Biochem.* **230,** 58–67.
11. Takeyasu, K., Omote, H., Nettikadan, S., Tokumasu, F., Iwamoto-Kihara, A. & Futai, M. (1996) *FEBS Lett.* **392,** 110–113.
12. Singh, S., Turina, P., Bustamante, C. J., Keller, D. J. & Capaldi, R. A. (1996) *FEBS Lett.* **397,** 30–34.
13. Stock, D., Leslie, A. G. & Walker, J. E. (1999) *Science* **286,** 1700–1705.
14. Zhang, Y., Oldenburg, M. & Fillingame, R. H. (1994) *J. Biol. Chem.* **269,** 10221–10224.
15. Zhang, Y. & Fillingame, R. H. (1995) *J. Biol. Chem.* **270,** 24609–24614.
16. Watts, S. D., Tang, C. & Capaldi, R. A. (1996) *J. Biol. Chem.* **271,** 28341–28347.
17. Hermolin, J., Dmitriev, O. Y., Zhang, Y. & Fillingame, R. H. (1999) *J. Biol. Chem.* **274,** 17011–17016.
18. Dimroth, P. (1997) *Biochim. Biophys. Acta* **1318,** 11–51.
19. Boyer, P. D. (1997) *Annu. Rev. Biochem.* **66,** 717–749.
20. Boyer, P. D. (1993) *Biochim. Biophys. Acta* **1140,** 215–250.
21. Boyer, P. D., Cross, R. L. & Momsen, W. (1973) *Proc. Natl. Acad. Sci. USA* **70,** 2837–2839.
22. Kayalar, C., Rosing, J. & Boyer, P. D. (1977) *J. Biol. Chem.* **252,** 2486–2491.
23. Boyer, P. D. & Kohlbrenner, W. E. (1981) in *Energy Coupling in Photosynthesis*, eds. Selman, B. & Selman-Reiner, S. (Elsevier/North–Holland, New York), pp. 231–240.
24. Duncan, T. M., Bulygin, V. V., Zhou, Y., Hutcheon, M. L. & Cross, R. L. (1995) *Proc. Natl. Acad. Sci. USA* **92,** 10964–10968.
25. Sabbert, D., Engelbrecht, S. & Junge, W. (1996) *Nature (London)* **381,** 623–625.
26. Noji, H., Yasuda, R., Yoshida, M. & Kinosita, K., Jr. (1997) *Nature (London)* **386,** 299–302.
27. Zhou, Y., Duncan, T. M., Bulygin, V. V., Hutcheon, M. L. & Cross, R. L. (1996) *Biochim. Biophys. Acta* **1275,** 96–100.
28. Zhou, Y., Duncan, T. M. & Cross, R. L. (1997) *Proc. Natl. Acad. Sci. USA* **94,** 10583–10587.
29. Kato-Yamada, Y., Noji, H., Yasuda, R., Kinosita, K., Jr. & Yoshida, M. (1998) *J. Biol. Chem.* **273,** 19375–19377.
30. Bulygin, V. V., Duncan, T. M. & Cross, R. L. (1998) *J. Biol. Chem.* **273,** 31765–31769.
31. Howitt, S. M., Rodgers, A. J., Hatch, L. P., Gibson, F. & Cox, G. B. (1996) *J. Bioenerg. Biomembr.* **28,** 415–420.
32. Vik, S. B., Long, J. C., Wada, T. & Zhang, D. (2000) *Biochim. Biophys. Acta* **1458,** 457–466.
33. Cross, R. L. (2000) *Biochim. Biophys. Acta* **1458,** 270–275.
34. Schulenberg, B., Aggeler, R., Murray, J. & Capaldi, R. A. (1999) *J. Biol. Chem.* **274,** 34233–34237.
35. Tsunoda, S. P., Aggeler, R., Yoshida, M. & Capaldi, R. A. (2001) *Proc. Natl. Acad. Sci. USA* **98,** 898–902. (First Published January 23, 2001; 10.1073/pnas.031564198)
36. Sambongi, Y., Iko, Y., Tanabe, M., Omote, H., Iwamoto-Kihara, A., Ueda, I., Yanagida, T., Wada, Y. & Futai, M. (1999) *Science* **286,** 1722–1724.
37. Tsunoda, S. P., Aggeler, R., Noji, H., Kinosita, K., Yoshida, M. & Capaldi, R. A. (2000) *FEBS Lett.* **470,** 244–248.
38. Jones, P. C., Hermolin, J., Jiang, W. & Fillingame, R. H. (2000) *J. Biol. Chem.* **275,** 31340–31346.
39. Hartzog, P. E. & Cain, B. D. (1994) *J. Biol. Chem.* **269,** 32313–32317.
40. Cox, G. B., Devenish, R. J., Gibson, F., Howitt, S. M. & Nagley, P. (1992) in *Molecular Mechanisms in Bioenergetics*, ed. Ernster, L. (Elsevier, New York), pp. 283–315.
41. Vik, S. B. & Antonio, B. J. (1994) *J. Biol. Chem.* **269,** 30364–30369.
42. Junge, W., Lill, H. & Engelbrecht, S. (1997) *Trends Biochem. Sci.* **22,** 420–423.
43. Jiang, W. & Fillingame, R. H. (1998) *Proc. Natl. Acad. Sci. USA* **95,** 6607–6612.
44. Dimroth, P., Wang, H., Grabe, M. & Oster, G. (1999) *Proc. Natl. Acad. Sci. USA* **96,** 4924–4929.
45. Rastogi, V. K. & Girvin, M. E. (1999) *Nature (London)* **402,** 263–268.
46. Hermolin, J. & Fillingame, R. H. (1995) *J. Biol. Chem.* **270,** 2815–2817.
47. Girvin, M. E., Hermolin, J., Pottorf, R. & Fillingame, R. H. (1989) *Biochemistry* **28,** 4340–4343.
48. Wise, J. G. (1990) *J. Biol. Chem.* **265,** 10403–10409.
49. Gibson, F., Downie, J. A., Cox, G. B. & Radik, J. (1978) *J. Bacteriol.* **134,** 728–736.
50. Gibson, F., Cox, G. B., Downie, J. A. & Radik, J. (1977) *Biochem. J.* **162,** 665–670.
51. Laemmli, U. K. (1970) *Nature (London)* **227,** 680–685.
52. Peterson, G. L. (1977) *Anal. Biochem.* **83,** 346–356.
53. Lotscher, H. R., deJong, C. & Capaldi, R. A. (1984) *Biochemistry* **23,** 4140–4143.
54. Watts, S. D. & Capaldi, R. A. (1997) *J. Biol. Chem.* **272,** 15065–15068.
55. Kimura, T., Suzuki, M., Sawai, T. & Yamaguchi, A. (1996) *Biochemistry* **35,** 15896–15899.
56. Jones, P. C., Jiang, W. & Fillingame, R. H. (1998) *J. Biol. Chem.* **273,** 17178–17185.
57. Jiang, W., Hermolin, J. & Fillingame, R. H. (2001) *Proc. Natl. Acad. Sci. USA* **98,** 4966–4971.
58. Hermolin, J. & Fillingame, R. H. (1989) *J. Biol. Chem.* **264,** 3896–3903.
59. Al-Shawi, M. K. & Nakamoto, R. K. (1997) *Biochemistry* **36,** 12954–12960.
60. Lundblad, R. L. (1991) *Chemical Reagents for Protein Modification* (CRC, Boca Raton, FL), 2nd Ed.